Practical Model for Tower Earthing Systems in Lightning Simulations

F. Koehler*, J. Swingler*

*School of Engineering & Physical Sciences, Heriot-Watt University, Edinburgh, EH14 4AS, UK, (fmk1@hw.ac.uk)

Abstract: In assessing the lightning performance of a transmission line with an Electromagnetic Transient (EMT) approach, the representation of the earthing system or tower footing can have a major impact on the simulation results. In this paper, a practical circuit for a direct implementation into an EMT software is presented, which uses a minimum of input parameters to represent a common four rod tower footing arrangement. Based on an available description of the frequency-dependency of a single rod in soil and a description of the ionization in soil for a single rod, a combined circuit model is developed for a tower earthing arrangement with four rods in a square arrangement. This approach takes into account the merging of the ionization zones from each rod.

Keywords: Lightning stroke; Lightning simulation; Transmission lines; Tower Earthing

1 Introduction

In the majority of performed studies to determine the lightning performance of a transmission line, a simple resistance model or variable resistance model is used [1]–[4]. This originates from the fact that in practice transmission codes state tower footing requirements (combined soil and electrode) as a resistance at power frequencies. Using formulas, such as from [5], the combined resistance of a tower earthing system and soil resistivity taken from measurements can be calculated. In the assessment of the lightning performance of a transmission line with an EMT approach

this type of modelling leads to conservative results due to the underestimation of the real performance of the earthing system [6].

However, several studies show that the frequency-dependency of soil has a major influence on the back-flashover rate of insulators and therefore should be included in lightning simulations [7], [8]. Furthermore, several studies show that the lightning performance of a tower is also very sensitive to the soil ionization process [9], [10]. Therefore these effects should also be included in simulations of lightning strikes to transmission lines. To simulate the behaviour of an earthing system subject to lightning impulses, models available in the literature are either based on electromagnetic field theory (EMF) [11]–[15], such as finite element methods (FEM) and Method of Moments (MoM), transmission line (TL) [16] or circuit theory [17]. Although EMF-based methods are the most accurate, computation time and complexity hinders the fast and simple simulation of a whole transmission line [18], but they are often used to verify circuit approaches or derive parameters for circuit elements, such as the pi-circuit based on EMF simulation results fitting in [19]. All these modelling approaches, lack the ease of a direct utilization in EMT simulations with a few input parameters.

In this paper, a practical model for tower foundations using so-called mini-piles is investigated, which are commonly employed in dense or rocky soil. This arrangement can be modelled with a four-rod in a square arrangement which features a high resistivity of the surrounding soil. Due to the general complexity of models, the soil ionization and frequency-dependent soil phenomena are separated in most simulation models and represented as a variable resistance or voltage/current source [20], [21]. In this paper both a frequency-dependent soil model and a single rod model available in the literature are combined, adapted and extended to model the four rod in a square arrangement. Since more than one rod is considered, a mathematical description of

both the dynamic mutual coupling as well as the dynamic merging of the ionization zones of the rods is proposed which uses only geometry parameters and low-frequency soil resistivity. Furthermore the model is verified with measurement results available in the literature.

2 Ionization Models

Although sole ionization models based on R-L-C circuits, such as in [22] feature a closer fit to some measurements, the overall performance differs only slightly from variable resistance models [23]. Therefore only variable resistance models for rods compatible to be included into circuits for frequency-dependency are considered. For a later comparison of the developed model in this paper, the similarity approach and CIGRE ionization model are taken as references.

2.1 Similarity Approach Ionization Model

A basic variable resistance model for a single rod, mentioned in [24], is based on Korsuncev similarity method with the dimensionless factors Π in (1) and (2). There, *s* is the distance between the center and the outermost point of the metallic structure in m, R_0 is the footing resistance in Ω, ρ is the soil resistivity in Ωm, *I* is the instantaneous current in kA and E_c is the breakdown electric field strength in kV/m. It is shown that a rod shaped electrode can be modelled as a hemispherical electrode shape with reasonable accuracy in (3), where *A* is the electrode surface area in m^2.

$$\Pi_1 = \frac{sR_0}{\rho} \tag{1}$$

$$\Pi_2 = \frac{\rho I}{E_c s^2} \tag{2}$$

$$\Pi_1^0 = 0.4517 + \frac{1}{2\pi} ln\left(\frac{s^2}{A}\right) \tag{3}$$

Furthermore, above a critical distance, the ionized zone can be simplified with a sphere electrode shape, where the correlation between Π_1 and Π_2 in the range of 0.3 to 10 for Π_2 in (4) can be applied.

$$\Pi_1 = 0.2631 \cdot \Pi_2^{-0.3082} \tag{4}$$

The resistive behaviour is now established with (1) and (3) until Π_1 in (4) is greater than Π_1^0 in (3), which is the criterion for the start of the ionization process. For a four rod arrangement, the total resistance is calculated with equations provided in the appendix of [25] and apply (1) and (3). The resulting variable footing resistance R_F as well as the derived critical current I_C where ionization starts, depend on a previously calculated total footing resistance R_0, in (5) and (6).

$$R_F = 0.2631 \frac{\rho}{s} \left(\frac{\rho I}{E_c l^2} \right)^{-0.3082} \tag{5}$$

$$\mathrm{I}_C = \frac{E_c s^2}{\rho} \left(\frac{\Pi_1}{0.2631} \right)^{\frac{1}{-0.3082}} \tag{6}$$

2.2 CIGRE Ionization Model

Another variable resistance model, such as proposed by Weck and adopted by CIGRE [26], takes into account the soil ionization effect in (7) and (8).

$$R_F = \frac{R_0}{\sqrt{1+\frac{I}{I_c}}} \tag{7}$$

$$I_c = \frac{E_c \rho}{2\pi {R_0}^2} \tag{8}$$

The model is developed for earthing rods and not meant to be for extensive earthing networks of more than 30m [27], such as counterpoise. The footing resistance can be calculated with formulas, such as in [28].

The determination of a generalized approach for the breakdown electric field strength remains difficult. In [29], various measurements are summarized and re-evaluated, which leads to a resistivity-dependent breakdown electric field strength ranging from 400 kV/m for 10 Ωm to 1750 kV/m for 10000 Ωm. For (2) an average of 1000 kV/m or the resistivity-dependent breakdown electric field strength from [29] is proposed. In [30] an investigation into previous experiments reported breakdown electric field strength is performed, which concludes to apply a value in the range of 300 kV/m to 400 kV/m. Other researchers [31], [32] confirm a value in the range of 300 kV/m to 400 kV/m, which is also the recommendation by CIGRE [27].

2.3 Shell Single Rod Ionization Model

A more elaborate soil ionization model for rods is based on the simplified physical description of the formation of the ionization zone in the form of conductive shells around the rod, as illustrated in Fig. 1, originally published by Liew and Darveniza [25] and later adapted and simplified by Nixon et al. [33] or changed to purely be based on physical constants by Cooray et al. [34].

As illustrated in Fig. 1, the ionization process starts at the rods surface, where the current density is the highest and streamers propagate in the direction away from the electrode until the electric field strength drops below the breakdown value [30]. The ionized zones in soil around the electrode increase the electrodes radius [27] and decrease the grounding system's resistance [28], [35]. For high soil resistivity the ionization process is more pronounced than for low soil resistivity [36]. In contrast to the sole current-dependent ionization models in section 2.1 and 2.2, this model features an additional time- or waveshape-dependency.

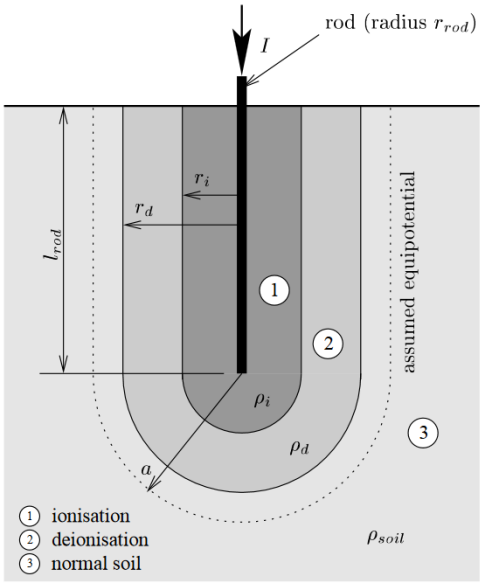

Fig. 1 Illustration of ionization and de-ionization zones of a rod electrode [37]

The mathematical description of a shell around the rod with radius a in m in (9) together with the various soil resistivities of each region, ionized, de-ionized and normal soil, enables the calculation of the total variable resistance.

$$dR = \frac{\rho}{2\pi l_{rod}}\left(\frac{1}{r_{rod}} - \frac{1}{a+l_{rod}}\right)da \tag{9}$$

As summarized in [25], [33] the following assumptions are made for the model:

- The soil surrounding the driven rod is homogeneous and isotropic with resistivity ρ_{soil}.
- An injected impulse current I in kA, results in equipotential surfaces that can be approximated by a cylindrical and hemispherical portion, as shown in Fig. 1.
- The current density J in kA/m^2, in the soil at a radial distance, r in m, from the center of the driven rod can be approximated by $J = \frac{I}{2\pi(r^2+rl_{rod})}$, where l_{rod} is the rod length in m.
- Breakdown by ionization occurs in the soil where the current density exceeds a critical value of current density, J_c, given by $J_c = \frac{E_c}{\rho_{soil}}$.

- The regions of ionization and de-ionization are assumed to be uniform as shown in Fig. 1 and the resistivity in these regions is time-varying.

The three different regions in Fig. 1 are calculated with soil resistivities in (10), where t_i is the onset time of ionization and τ_i the ionization constant and t_d is the de-ionization onset time, τ_d the de-ionization constant, all in unit seconds, and ρ_m the soil resistivity at the onset of de-ionization in Ωm.

Region 1: $$\rho_i = \rho_{soil} \cdot e^{\frac{-t_i}{\tau_i}} \quad J \geq J_c \quad r_{rod} < r \leq r_i$$

Region 2: $$\rho_d = \rho_m + \left(\rho_{soil} - \rho_m\right)\left(1 - e^{\frac{-t_d}{\tau_d}}\right)\left(1 - \frac{J}{J_c}\right)^2 \quad J < J_c \quad r_i < r \leq r_d \qquad (10)$$

Region 3: $$\rho_{soil} \quad J < J_c \quad r > r_d$$

Liew and Darveniza express the total resistance as an integral, where an approximation for the total resistance during the ionization process in (11) is provided by Nixon et al. [33].

$$R_F = \frac{\rho_i}{2\pi l_{rod}} \ln \frac{r_i(r_{rod}+l_{rod})}{r_{rod}(r_i+l_{rod})} + \frac{\rho_d}{2\pi l_{rod}} \ln \frac{r_d(r_i+l_{rod})}{r_i(r_d+l_{rod})} + \frac{\rho_{soil}}{2\pi l_{rod}} \ln \frac{r_d+l_{rod}}{r_d} \qquad (11)$$

In case of no ionization, the steady-state resistance for a single rod is given in (12) by Liew and Darveniza [25], which represents the case of r_i=0 and r_d=r_{rod}.

$$R_F = \frac{\rho_{soil}}{2\pi l_{rod}} \ln \frac{r_{rod}+l_{rod}}{r_{rod}} \qquad (12)$$

3 Frequency-Dependent Soil Model

In [38] modelling of the frequency-dependency of soil for rod geometries with an R-C-circuit is performed. The circuit in Fig. 2 comprises an R-C-element for low- and high-frequency-response of soil as well as a resistance for the initial impulse response. The traveling wave phenomenon is neglected due to the short length of rods, but the initial surge response is included.

The calculation of the circuits parameters is readily performed with the geometry factor for rods in [5], using solely the soil low-frequency resistivity and rod geometry values. First, the steady-state parameters including the surge impedance are calculated in (13) to (16), where l and r are the length and outer radius of the rod electrode in m, ρ_0, $\varepsilon_0$and μ_0 are the low-frequency soil resistivity in Ωm, permittivity in F/m and permeability in H/m.

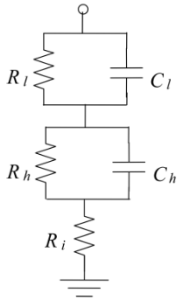

Fig. 2 Equivalent RC-circuit for frequency-dependent low-current earthing rod modelling

$$K = \frac{1}{2\pi l}\ln\frac{l+r}{r} \tag{13}$$

$$R_0 = \rho_0 \mathrm{K} \tag{14}$$

$$C_0 = \varepsilon_0 \mathrm{K}^{-1} \tag{15}$$

$$Z_0 = \sqrt{\frac{\mu_0 l^2 K^2}{\varepsilon_0}} \tag{16}$$

The impulse resistance R_i is calculated according to [38], [39] for the case of the sending end voltage neglecting damping for short rod arrangements in (17).

$$R_i = 3Z_0 \cdot \left(\exp\left(-\frac{Z_0}{R_0}\right)\right)^2 \tag{17}$$

The high-frequency circuit is calculated with (18) to (20) at $f_h = 100\ \mathrm{kHz}$ due to the range of rise-times of first negative lightning strike current in the microsecond range

[40] using the frequency-dependent soil formulas from (21) and (22) to determine soil resistivity $\rho_r(f_h) = \frac{\rho}{\rho_0}$ and permittivity $\varepsilon_r(f_h)$.

$$\tau_h = \rho_0 \rho_r(f_h) \varepsilon_0 \varepsilon_r(f_h) \tag{18}$$

$$R_h = R_0 \cdot \rho_r(f_h) - R_i \tag{19}$$

$$C_h = \frac{\tau_h}{R_h} \tag{20}$$

The frequency-dependent formulas for soil resistivity and permittivity from [41] are utilized in (21) and (22), which satisfy the Kramers–Kronig relationship and represent a causal model in comparison to the formulas used in [38].

$$\rho = \left(\sigma_0 + \sigma_0 \cdot h(\sigma_0) \left(\frac{f}{1MHz}\right)^{\gamma}\right)^{-1} \tag{21}$$

$$\varepsilon_r = \varepsilon_{r\infty} + \frac{\tan(\pi\gamma/2) \cdot 10^{-3}}{2\pi\varepsilon_0 (1MHz)^{\gamma}} \sigma_0 \cdot h(\sigma_0) f^{\gamma - 1} \tag{22}$$

σ is the soil conductivity in mS/m, σ_0 the low-frequency soil conductivity (100Hz) in mS/m, $h(\sigma_0) = 1.26 \cdot \sigma_0^{-0.73}$, f the frequency in Hz, $\gamma = 0.54$, ε_r the relative permittivity, $\varepsilon_{r\infty} = 12$ the relative permittivity at high frequencies and $\varepsilon_0 \cong 8.854 \cdot 10^{-12}$F/m, the vacuum permittivity.

The low-frequency circuit is calculated with (23) to (25) at $f_l = 100$ Hz, the lowest possible value for equation in (19) and (20) for determination of $\rho_r(f_l)$ and $\varepsilon_r(f_l)$.

$$\tau_l = \rho_0 \varepsilon_0 \varepsilon_r(f_l) \tag{23}$$

$$R_l = R_0 - R_i - R_h \tag{24}$$

$$C_l = \frac{\tau_l}{R_l} \tag{25}$$

4 Combined Frequency-Dependent Soil and Ionization Models

4.1 Single Rod Model

In [38], it is mentioned that soil ionization can be included in the initial surge resistance R_i of the described frequency-dependent model. However, the presented ionization models are all based on the calculation of the steady-state resistance R_0, rather than the initial surge resistance. Therefore, a decrease of R_i will not result in the same degree of voltage reduction as a decrease of the steady-state resistance R_0. Furthermore, the idea to decrease R_i based on the ratio of R_i/R_0 is only valid for $R_i > 0$. Therefore, the approach is taken to vary all resistance values in the circuit. Since the frequency-dependent effect is negligible when the ionization effect is present above a certain threshold, the change of resistance with respect to the frequency-dependent part of the circuit does not affect the overall behaviour. To incorporate soil ionization into the R-C-circuit model, a dynamic calculation of all circuit element values and variable resistance elements have to be included in the circuit. For the recalculation of R-values the steady-state resistance R_0 is varied, according to the ionization model.

4.2 Four Rods in a Square Model

As mentioned in the introduction, a typical mini-pile tower foundation for transmission towers is investigated. Since a mini-pile tower foundation comprises four steel-reinforced cores, each encased in concrete and electrically connected through the tower feet, it is decided to simplify this arrangement to a rod-like geometry. Although the concrete, which encases the steel reinforcement, has a different soil resistivity than the surrounding soil, this effect is neglected. In [42] formulas are provided to include this effect, but as shown [43] the impedance of concrete is lower than most soil and thus the simplification is a worst-case approximation. The geometry and associated distances of the investigated arrangement are illustrated in Fig. 3. Typical

values for *d* for towers with mini-pile foundations are between 4 and 12 m with depth *l* between 1 m and 5 m and thickness of 0.3 m to 0.8 m.

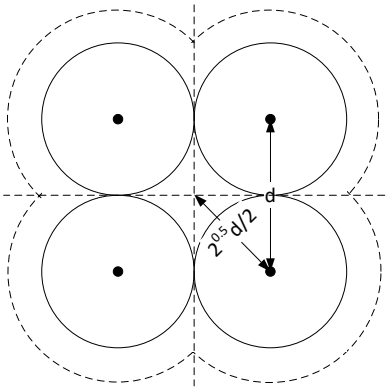

Fig. 3 Illustration of four rods in a square

Since the frequency-dependent parameters are based on the geometry parameter K and the four rods are electrically connected in parallel at the tower base, the mathematical calculation of the frequency-dependent circuit remains the same but considers the mutual coupling between the four rods in (26), replacing (13) in the frequency-dependent circuit calculation.

$$K = \frac{1}{8\pi l}\left(4\ln\frac{l+r}{r} + 2\ln\left(\frac{2l+\sqrt{d^2+4l^2}}{d}\right) + \frac{d}{2l} - \frac{\sqrt{d^2+4l^2}}{2l} + \ln\left(\frac{2l+\sqrt{(\sqrt{2}d)^2+4l^2}}{(\sqrt{2}d)}\right) + \frac{(\sqrt{2}d)}{2l} - \frac{\sqrt{(\sqrt{2}d)^2+4l^2}}{2l}\right) \quad (26)$$

For the ionization phenomenon Liew and Darveniza [25] already proposed an area criterion in (27) to (29) for the four rod arrangement in Fig. 3.

$$R_F = \frac{1}{4}\int_{r_0}^{\infty}\frac{\rho}{A_1+A_2}\,dr \quad (27)$$

There, the cylindrical and sphere shape surfaces of the ionization zones can be described with (28) and (29), where $\theta = \cos^{-1}\frac{d}{2r}$.

$$\begin{aligned} A_1 &= 2\pi rl & r_0 < r \le d/2 \\ A_1 &= (2\pi - 4\theta)rl & d/2 < r \le \sqrt{2}d/2 \\ A_1 &= \left(\frac{3}{2}\pi - 2\theta\right)rl & \frac{\sqrt{2}d}{2} < r \le \infty \end{aligned} \quad (28)$$

$$\begin{aligned} A_2 &= 2\pi r^2 && r_0 < r \leq d/2 \\ A_2 &= \pi r d && d/2 < r \leq \frac{\sqrt{2}d}{2} \\ A_2 &= \pi r d + r^2\theta(\sin\theta - \cos\theta) && \frac{\sqrt{2}d}{2} < r \leq \infty \end{aligned} \tag{29}$$

To determine the expansion of the ionization areas of the four rod arrangement a dynamic calculation of the ionization radius is necessary. The ionization radius needs to be solved for the three cases of the ionized area of each rod with (30). Since the rods are connected in parallel at the tower base, the current I flowing from the tower to ground is quartered.

$$J = \frac{I}{A} \xrightarrow{yields} J = \frac{I}{4 \cdot A_{rod}} \xrightarrow{yields} J = \frac{I}{4 \cdot (A_1 + A_2)} \tag{30}$$

Up to $d/2$ in Fig. 3, the ionization radius is calculated for each rod separately. At $d/2$ the ionization areas merge and thus the ionization area needs to be adjusted. From $\sqrt{2}d/2$ onwards the total ionization area only expands at the outer borders until infinity, which is the similarity case of a sphere electrode.

Solving (30) for the case of $r_0 < r \leq d/2$, the radius can easily be determined with the 2nd order equation in (31). The formula is the same as for a single rod, adjusted with a division of the current by four.

$$r_1 = \frac{1}{2}\left(-l + \sqrt{l^2 + \frac{I}{2\pi J_c}}\right) \tag{31}$$

Although Liew and Darveniza [25] provides the mathematical description for $d/2 < r \leq \sqrt{2}d/2$, the arising problem with the solution of the resulting equation due to the arccosine description of the angle θ in (32) is not addressed.

$$2\pi r l - 4 r l \theta \ + \pi r d - \frac{I}{4 J_{ion}} = 0 \tag{32}$$

A plot of $d/2 < r \leq \sqrt{2}d/2$ as an input to (32) and inverse of axis shows the mathematical problem in more detail in Fig. 4 with an example. The function $r_2(I)$ would feature two y-axis values for one x-axis value, which prevents a direct solution and an approximation has to be determined. As noticed in Fig. 4, the increase in radius is approximately linear with high soil resistivities. Furthermore, the expansion of the radius up to $d/2$ demands higher currents with increasing soil resistivity.

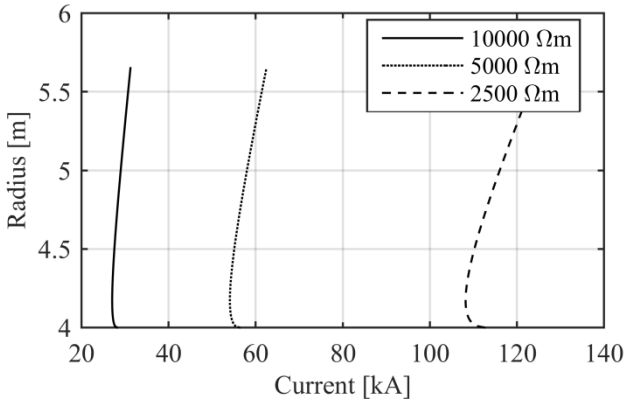

Fig. 4 Ionization current vs radius for four rods in parallel, $d = 8$ m, $r_{rod} = 0.1$ m, $l_{rod} = 3$ m and $E_c = 400$ kV/m in the range $d/2 < r \leq \sqrt{2}d/2$

Since the highest lightning stroke currents are in the range of 350 kA [44] and are distributed among shield wires and tower footing, only soil resistivities above 2500 Ωm in this configuration feature a merging of ionization zones. Therefore a linearization of the radius with a first order function is justified in this case. Solving (32) for $r = d/2$ and $r = \sqrt{2}/2\ d$ gives the two points for linearization in (33).

$$\begin{aligned} r &= \frac{d}{2} & 2\pi J_{ion}(d^2 + 2dl) &= I \\ r &= \frac{\sqrt{2}}{2}d & 2\sqrt{2}\pi J_{ion}(dl + d^2) &= I \end{aligned} \tag{33}$$

The ionization radius $r_2(I)$ is then calculated by determination of the slope and offset of the term $I(r) = m \cdot r + t$ and solved for r in (34).

$$r_2 = \frac{\frac{I}{\pi J_{ion}}(\sqrt{2}-1)-dl\sqrt{2}}{4\left(l(\sqrt{2}-2)+d(\sqrt{2}-1)\right)} \tag{34}$$

Furthermore, for $r > \sqrt{2}d/2$ a linearization of the equation to solve for radius r_3 in (35) is necessary.

$$\left(\frac{3}{2}\pi - 2\theta\right) rl + 2\pi r^2 \cos\theta + r^2\theta(\sin\theta - \cos\theta) - \frac{I}{4J_{ion}} = 0 \tag{35}$$

A plot of $(\sqrt{2}\ d)/2\ \ < r \leq \infty$ as an input to (35) and inverse of axis in Fig. 5 shows the curve progression for three soil resistivities for an example configuration. For the selected soil resistivities, the curves tend to be linear up to the footing distance d, which is more pronounced for higher soil resistivities. Furthermore, from a numerical viewpoint, the development of a linearization including ∞ is not possible.

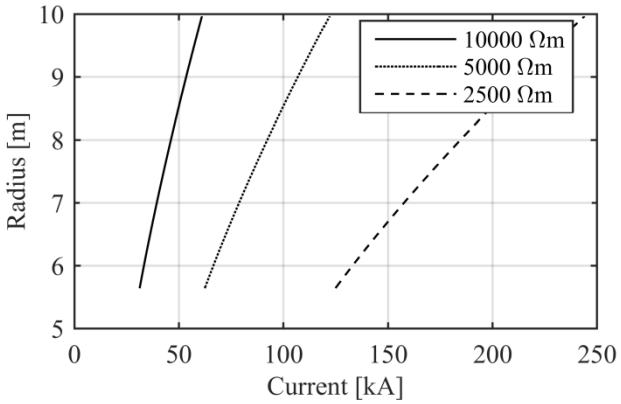

Fig. 5 Ionization current vs radius for four rods in parallel, $d = 8$ m, $r_{rod} = 0.1$ m, $l_{rod} = 3$ m and $E_c = 400$ kV/m in the range $(\sqrt{2}\ d)/2 < r \leq \infty$

Derived from the trend of a linear progression of ionization radius in dependency of the current for higher soil resistivities and necessary higher currents to achieve the same ionization radius for lower soil resistivities, the starting value of $(\sqrt{2}\ d)/2$ and the distance d are chosen for linearization. With the linearization points $r = d$ in (36) and $r = \sqrt{2}/2\ d$ in (35), the slope and offset can be determined as in the previous case.

$$r = d \quad \frac{5}{6}dl + d^2 + d^2\frac{1}{3}\left(\frac{\sqrt{3}}{2} - \frac{1}{2}\right) = \frac{I}{4\pi J_{ion}} \tag{36}$$

The resulting formula for the radius r_3 is given in (37) to (39).

$$r_3 = \frac{I-t}{m} \tag{37}$$

$$m = \left(4\pi J_{ion}\left(\frac{5}{6}l + d + d\frac{1}{3}\left(\frac{\sqrt{3}}{2} - \frac{1}{2}\right)\right) - 2\sqrt{2}\pi J_{ion}(l+d)\right) / \left(1 - \frac{\sqrt{2}}{2}\right) \tag{38}$$

$$t = 4\pi J_{ion}\left(\frac{5}{6}dl + d^2 + d^2\frac{1}{3}\left(\frac{\sqrt{3}}{2} - \frac{1}{2}\right)\right) -$$

$$\left(4\pi J_{ion}\left(\frac{5}{6}dl + d^2 + d^2\frac{1}{3}\left(\frac{\sqrt{3}}{2} - \frac{1}{2}\right)\right) - 2\sqrt{2}\pi J_{ion}d(l+d)\right) / \left(1 - \frac{\sqrt{2}}{2}\right) \tag{39}$$

A graphical illustration of the equivalent ionization radii comprised of the cylinder and sphere parts for a practical example is shown in Fig. 6 in dependency of the injected current.

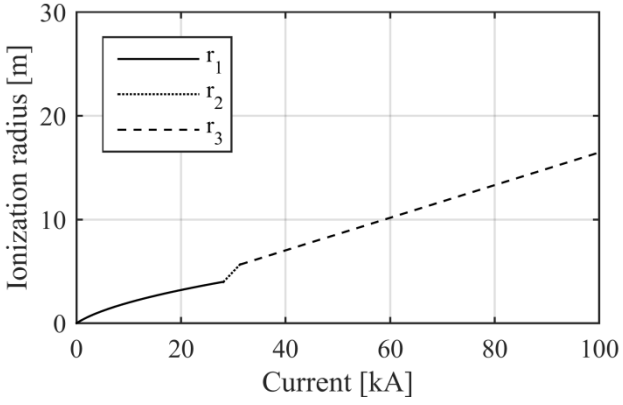

Fig. 6 Ionization current vs radius for four rods in parallel, $d = 8$ m, $r_{rod} = 0.1$ m, $l_{rod} = 3$ m, $\rho = 10000$ Ωm and $E_c = 400$ kV/m

The plot shows the effect of the merging of the four different ionization zones, as from the intersection of radius r_1 and r_2 nearly no increase of the radius is achieved. At a point where all four ionization zones fully merge into one, the increase is

approximately equivalent to the increase of a sphere electrode as discussed in the similarity approach.

The practical implementation of the developed formulation of the merging of ionization zones into the frequency-dependent circuit however faces some challenges when (27) is applied to an EMT calculation. Due to the nature of the integral in (27) and the dynamic ionization radi calculation, a sum of up to nine integrals, each using the trapezoidal rule to calculate the areas of ionization, deionization and no ionization for each tower foot has to be calculated for each time-step in the simulation. In a Monte-Carlo simulation with a considerable number of towers this leads to a significant increase in simulation time.

Therefore, in this work, an alternative model is proposed to calculate the dynamic resistance of a four rod in a square arrangement with (26), which includes the description for a single rod as well as the mutual coupling to the other rods. From measurements of a four rod arrangement [31], it is known, that the mutual resistance is only reduced slightly. It is concluded as a worst-case approximation that the mutual impedance remains constant. To include the merging of the ionization zones, the part of the equation describing the single rod in (26) is replaced with (11) and the mathematical description of the radi from (31), (34) and (37) is applied for the expanding ionization zone.

The whole developed model featuring soil frequency-dependency and soil ionization then consists of an initial calculation of the R-C circuit parameters in Fig. 2 using (14) to (26). The ionization is built into the model through the implementation of (11) in (26) and (10), which are used to calculate the change of R_0 and subsequently the change of R_h, R_l and R_i in the R-C-circuit during ionization.

5 Model Verification

5.1 Single Rod Ionization Model

To validate the implementation of the developed calculation routine and investigate the difference to the similarity approach and CIGRE soil ionization model, simulation results from Nixon et al. [37] are utilized, which feature realistic lightning waveshapes in lab tests (3.5-5/10-14 µs at 5/29 kA) and feature a good agreement with original results from Liew and Darveniza [25] for soil resistivities in the range of 50 Ωm to 3100 Ωm. The described rod geometry and model parameters from [37] are given in Table 1.

Table 1 :Soil and Electrode Parameters in Nixon's Lab Experiments

ρ in Ωm	139
E_0 in kV/m	300
τ_i in µs	2.0
τ_d in µs	4.5
r_{rod} in mm	7.95
l_{rod} in mm	2667

For the similarity approach and CIGRE model the recommended 1000 kV/m and 400 kV/m critical electric field strength are applied in the model. Nixon et al. [33] (11) verified his model with two applied current waveforms to a single rod, as depicted in Fig. 7, implemented in PSCAD/EMTDC. The resulting resistance of the model and, for comparison, the similarity approach and CIGRE model is plotted in Fig. 8.

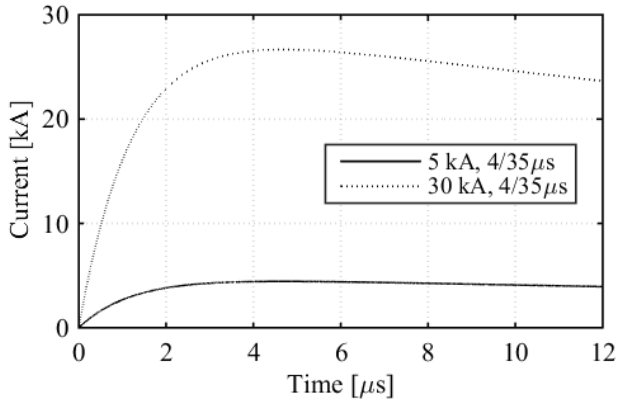

Fig. 7 Current waveforms used in lab investigation in [37], implemented in PSCAD/EMTDC

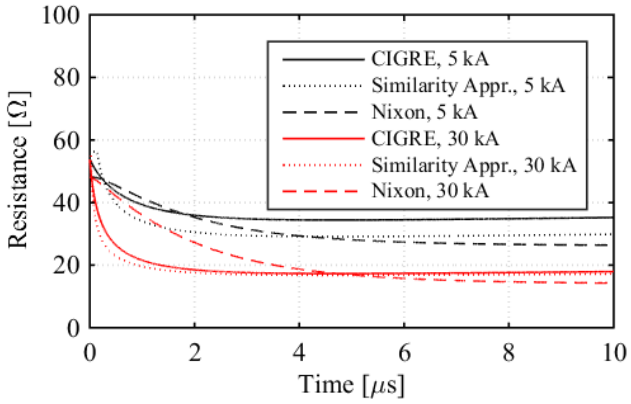

Fig. 8 Simulation results from PSCAD/ETMDC of soil ionization models according to Nixon et al. [37], similarity approach [24] and CIGRE [26] for a single rod

A comparison of the simulation results for the Nixon model to its reference [37] shows that only marginal differences to the PSCAD/EMTDC implementation exist. These differences are attributed to the waveform generation. Furthermore, a comparison of the similarity approach, CIGRE and shell model resistance progression in the simulation in Fig. 8 reveals that the similarity approach and CIGRE models initial resistance decrease is more progressive than in Nixon's model. This originates from the modeling of the ionization and de-ionization process in the shell model. However, the overall reduction of resistance is more pronounced in Nixon's model afterwards. This is due to

the different equations used for calculating the initial footing resistance, as summarized in Table 2.

Table 2: Low-Frequency Footing Resistances

Similarity approach with (1)/(3) in Ω	56
CIGRE model with (13)/(14) in Ω	54
Nixon model with (11) in Ω	48

5.2 Frequency-Dependent Soil Model

For the verification of the described frequency-dependent circuit in combination with the ionization model in the low current impulse range, measurement results of an earthing rod in [31] are utilized. The corresponding simulation parameters are summarized in table 3. For the generation of lightning impulses, the current generator circuit used in the measurements is modelled according to [45]. The simulation results for a single rod in 160 Ωm soil subject to lightning impulses with current amplitudes of 0.51 kA/ 0.81 kA/1.13 kA are depicted in Fig. 9.

Table 3: Soil and Electrode Parameters in Sekioka's Lab Experiments

ρ in Ωm	160
E_0 in kV/m	300
r_{rod} in mm	7.00
l_{rod} in mm	1500

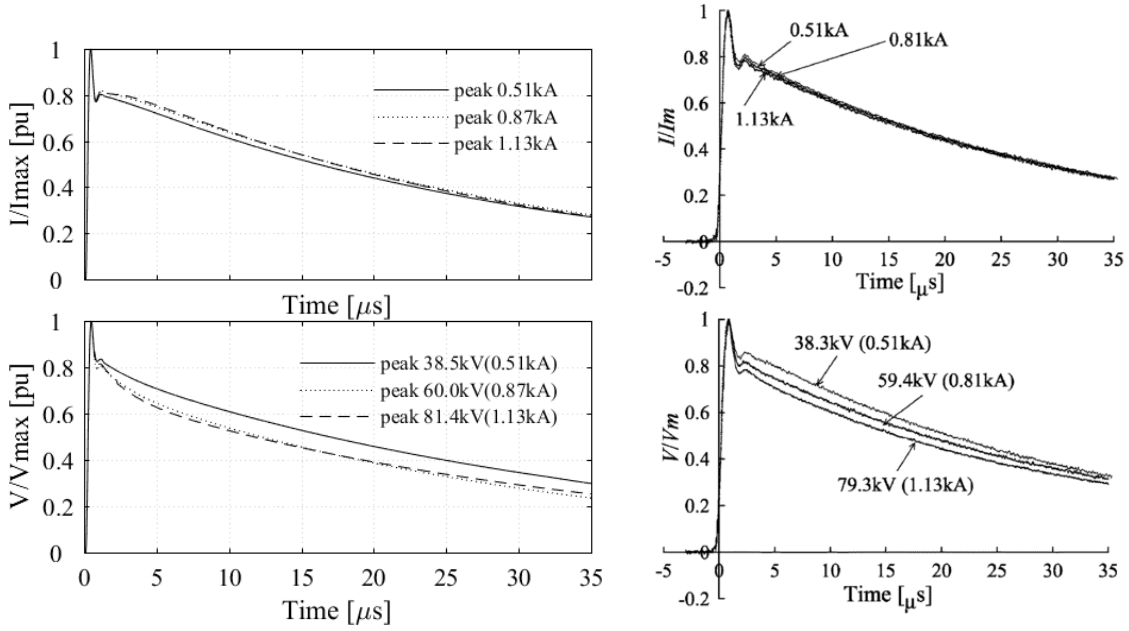

(a) PSCAD/EMTDC simulation (b) Measurements from Sekioka [31]

Fig. 9 Validation of frequency-dependent model according to Sekioka [31] and shell ionization model [37], lightning impulse to single rod in 160 Ωm soil

A comparison of the PSCAD/EMTDC simulation results to the reference [31] shows a good agreement. Therefore, it can be concluded, that the adjusted frequency-dependent model in combination with the shell ionization model can be used to model both soil ionization and frequency-dependent behaviour of single rods. Furthermore, this represents a further verification of the Nixon ionization model with measurements.

5.3 Combined Model for Four Rods in a Square

Although measurements of the ionization and frequency-dependent behaviour of four rods in a square are conducted in [31] and [25], the soil resistivity is too low to result in a merging of the ionization zones. However verification on the basis of the similarity and the CIGRE model can be accomplished and the overall influence on resulting voltage assessed. The simulation results for a negative first and subsequent stroke [46], applied to the developed model of merging ionization zones of a practical tower footing configuration are shown in Fig. 10 and Fig 11.

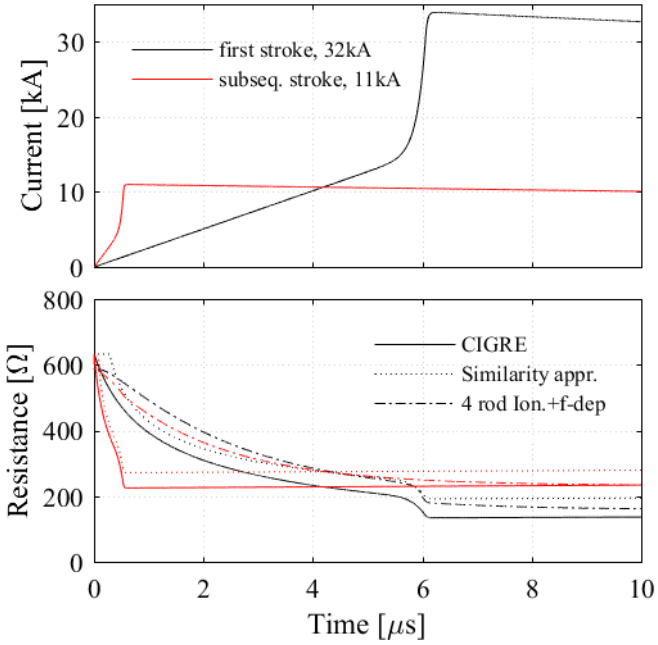

Fig. 10 Simulation results of median strokes to advanced frequency-dependent soil model with ionization for four rods in parallel, $r_{rod} = 0.1$ m, $l_{rod} = 3$ m, d=8 m, $\rho =$ 10000 Ωm

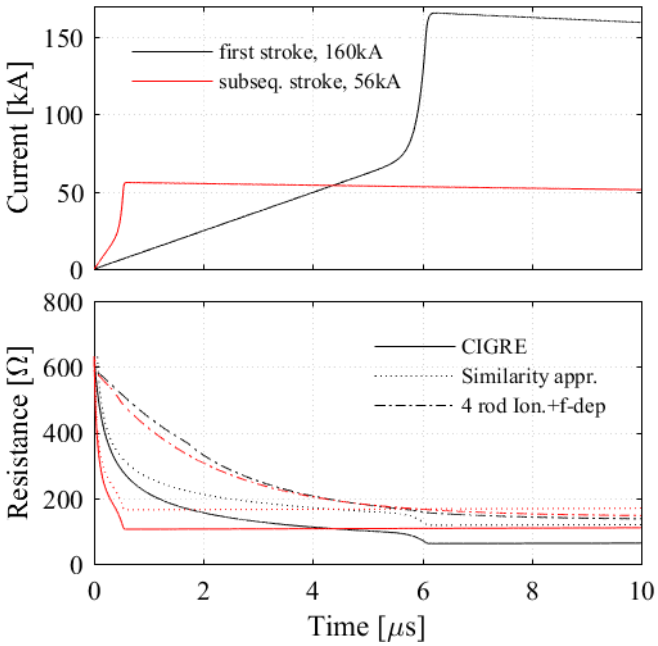

Fig. 11 Simulation results of severe strokes to advanced frequency-dependent soil model with ionization for four rods in parallel, $r_{rod} = 0.1$ m, $l_{rod} = 3$ m, d=8 m, $\rho =$ 10000 Ωm

The comparison of progression of resistance for CIGRE, similarity approach and the developed model for a negative first stroke shows a very similar behaviour with regard

to the reduction of resistance. For the negative subsequent stroke the time delay in the shell model is more dominant, leading to a slower reduction in resistance over time. However the minimum resistance value is very similar to the other models. Furthermore, the resistance progression of the similarity approach and the developed model converge with increasing current, as seen in the case of severe strokes in Fig. 11. The reason for this is that with increasing current the merging of ionization zones forms a spherical area, which is both taken into account in the similarity approach and the developed model.

6 Summary and Conclusion

In this paper, an extension to the Nixon ionization model for earthing rods is developed, which takes into account the merging of ionization zones in practical tower earthing systems with four rods at higher soil resistivities or higher currents. Furthermore, based on Sekioka's circuit approach to model the soil frequency-dependency of earthing rods, a rod model considering frequency-dependency of soil and ionization effect is developed. Based on measurements found in the literature, the developed model is verified with simulations in PSCAD/EMTDC. A comparison of the developed model to the CIGRE and similarity approach model is performed for verification purpose of the tower footing with four rods, because no measurements at higher soil resistivities are available in the literature. The tower configuration of an extreme case, where merging of the ionization zones takes place, shows that CIGRE, similarity approach and the developed model in this work show a very similar behaviour for first strokes. For higher currents the similarity approach and developed model resistance progression converge due to the merge of ionization zones forming a hemispherical shape. For subsequent strokes the minimum resistance value during ionization is also very similar for all three models, but due to the incorporated time

delay in the developed ionization model, the reduction of resistance is slower and thus overvoltages at insulators are higher. Especially this phenomenon is pronounced for severe strokes with a very short rise-time. From this it can be concluded that in the simulation of subsequent strokes to an overhead line using the developed tower footing model, the resulting initial overvoltages at the insulator strings are higher than those where the CIGRE or similarity approach model is taken into account. This is aligned with conclusions in [47], where it is concluded that the tower grounding model practically does not influence the overvoltages at the insulator strings generated by subsequent strokes.

In conclusion, the developed model offers the benefit of a more conservative approach to the grounding system ionization behaviour than the CIGRE and similarity approach model with regard to subsequent strokes and maintains the expected behaviour for first strokes. Furthermore, due to the simplified description of the four rod arrangement in high soil resistivities without integration over the radius and suitable behaviour for both first and subsequent stroke rise-times, it is compatible with an EMT Monte-Carlo approach.

7 Acknowledgement

This work is supported by Faiva Wadawasina of Scottish and Southern Electricity Networks, Perth, Scotland (SSEN) under the OFGEM Network Innovation Allowance (NIA_SHET_0011).

8 References

[1] A. Ametani and T. Kawamura, “A method of a lightning surge analysis recommended in Japan using EMTP,” *IEEE Transactions on Power Delivery*, vol. 20, no. 2 I, pp. 867–875, 2005.

[2] CIGRE Working Group 33.02, “Guidelines for Representation of Network Elements when Calculating Transients,” 1990.

[3] N. Filipe, C. Cardoso, J. Mendes, D. Duarte, L. Perro, and M. M. Fernandes, “A methodology for estimating transmission lines lightning performance using a statistical approach,” in *International Conference on Lightning Protection*, 2016.

[4] Z. Datsios and P. Mikropoulos, “Implementation of leader development models in ATP-EMTP Using a type-94 circuit component,” *International Conference on Lightning Protection*, 2014.

[5] H. B. Dwight, “Calculation of Resistances to Ground,” *Electrical Engineering*, no. December, 1936.

[6] J. Wu, J. He, B. Zhang, and R. Zeng, “Influence of grounding impedance model on lightning protection analysis of transmission system,” *Electric Power Systems Research*, vol. 139, no. JANUARY, pp. 133–138, 2016.

[7] S. Visacro and F. H. Silveira, “The Impact of the Frequency Dependence of Soil Parameters on the Lightning Performance of Transmission Lines,” *IEEE Transactions on Electromagnetic Compatibility*, vol. 57, no. 3, pp. 434–441, 2015.

[8] S. Visacro, R. Alipio, M. H. Murta Vale, and C. Pereira, “The response of grounding electrodes to lightning currents: The effect of frequency-dependent soil resistivity and permittivity,” *IEEE Transactions on Electromagnetic Compatibility*, vol. 53, no. 2, pp. 401–406, 2011.

[9] M. Fernandes, M. C. de Barros, and M. Ameida, “Statistical Study of the Lightning Overvoltages at a Gas Insulated Station Transformer,” *International Conference on Power Systems Transients*, 1995.

[10] N. Harid, H. Griffiths, N. Ullah, M. Ahmeda, and A. Haddad, “Experimental investigation of impulse characteristics of transmission line tower footings,”

Journal of Lightning Research, pp. 36–44, 2012.

[11] L. D. Grcev and F. Dawalibi, “An electromagnetic model for transients in grounding systems,” *IEEE Transactions on Power Delivery*, vol. 5, no. 4, pp. 1773–1781, 1990.

[12] L. D. Grcev, “Computer analysis of transient voltages in large grounding systems,” *IEEE Transactions on Power Delivery*, vol. 11, no. 2, pp. 815–823, 1996.

[13] K. Tanabe and A. Asakawa, “Computer analysis of transient performance of grounding grid element based on the finite-difference time-domain method,” *International Symposium on Electromagnetic Compatibility*, vol. 1, p. 209–212 Vol.1, 2003.

[14] R. Xiong, B. Chen, C. Gao, Y. Yi, and W. Yang, “FDTD calculation model for the transient analyses of grounding systems,” *IEEE Transactions on Electromagnetic Compatibility*, vol. 56, no. 5, pp. 1155–1162, 2014.

[15] J. Wu, B. Zhang, J. He, R. Zeng, and S. Member, “A Comprehensive Approach for Transient Performance of Grounding System in the Time Domain,” *IEEE Transactions on Electromagnetic Compatibility*, vol. 57, no. 2, pp. 250–256, 2015.

[16] C. Mazzetti and G. M. Veca, “Impulse Behavior of Ground Electrodes,” *IEEE Power Engineering Review*, vol. PER-3, no. 9, p. 46, 1983.

[17] R. Velazquez and D. Mukhedkar, “Analytical Modelling of Grounding Electrodes Transient Behavior,” *IEEE Transactions on Power Apparatus and Systems*, vol. PAS-103, no. 6, pp. 1314–1322, 1984.

[18] L. Grcev, “Time- and frequency-dependent lightning surge characteristics of grounding electrodes,” *IEEE Transactions on Power Delivery*, vol. 24, no. 4, pp. 2186–2196, 2009.

[19] P. Yutthagowith, “A Modified Pi-Shaped Circuit-Based Model of Grounding Electrodes,” in *International Conference on Lightning Protection*, 2016.

[20] M. Mokhtari, Z. Abdul-Malek, and Z. Salam, “An Improved Circuit-Based Model of a Grounding Electrode by Considering the Current Rate of Rise and Soil Ionization Factors,” *IEEE Transactions on Power Delivery*, vol. PP, no. 99, pp. 1–1, 2014.

[21] F. M. Gatta, A. Geri, S. Lauria, and M. Maccioni, “Generalized pi-circuit tower grounding model for direct lightning response simulation,” *Electric Power Systems Research*, vol. 116, pp. 330–337, 2014.

[22] N. Mohamad Nor, A. Haddad, and H. Griffiths, “Characterization of ionization phenomena in soils under fast impulses,” *IEEE Transactions on Power Delivery*, vol. 21, no. 1, pp. 353–361, 2006.

[23] E. P. Nicolopoulou, F. E. Asimakopoulou, I. F. Gonos, and I. a. Stathopulos, “Comparison of circuit models for the simulation of soil ionization,” *International Conference on Lightning Protection*, no. 1, pp. 1–6, 2012.

[24] W. A. Chisholm and W. Janischewskyj, “Lightning surge response of ground electrodes,” *IEEE Transactions on Power Delivery*, vol. 4, no. 2, pp. 1329–1337, 1989.

[25] A. C. Liew and M. Darveniza, “Dynamic model of impulse characteristics of concentrated earths,” *Proceedings of the Institution of Electrical Engineers*, vol. 121, no. 2, p. 123, 1974.

[26] CIGRE Working Group 33.01, “Guide to procedures for estimating the lightning performance of transmission lines,” 1991.

[27] A. Geri, “Behaviour of grounding systems excited by high impulse currents: the model and its validation,” *IEEE Transactions on Power Delivery*, vol. 14, no. 3, pp. 1008–1017, 1999.

[28] R. Ruedenberg, “Grounding principles and practice I—Fundamental considerations on ground currents,” *Electrical Engineering*, vol. 64, no. 1, pp. 1–13, 1945.

[29] E. E. Oettle, “A new general estimation curve for predicting the impulse impedance of concentrated earth electrodes,” *IEEE Transactions on Power Delivery*, vol. 3, no. 4, pp. 2020–2029, 1988.

[30] A. M. Mousa, “The soil ionization gradient associated with discharge of high currents into concentrated electrodes,” *IEEE Transactions on Power Delivery*, vol. 9, no. 3, pp. 1669–1677, 1994.

[31] S. Sekioka, T. Sonoda, and a. Ametani, “Experimental Study of Current-Dependent Grounding Resistance of Rod Electrode,” *IEEE Transactions on Power Delivery*, vol. 20, no. 2, pp. 1569–1576, 2005.

[32] R. E. de Souza, F. H. Silveira, and S. Visacro, “The effect of soil ionization on the lightning performance of transmission lines,” *International Conference on Lightning Protection*, pp. 1307–1311, 2014.

[33] K. J. Nixon, I. R. Jandrell, and A. J. Phillips, “A simplified model of the lightning performance of a driven rod earth electrode in multi-layer soil that includes the effect of soil ionisation,” *Conference Record - IAS Annual Meeting (IEEE Industry Applications Society)*, vol. 4, no. c, pp. 1821–1825, 2006.

[34] V. Cooray, M. Zitnik, M. Manyahi, R. Montano, M. Rahman, and Y. Liu, “Physical model of surge-current characteristics of buried vertical rods in the presence of soil ionisation,” *Journal of Electrostatics*, vol. 60, no. 2–4, pp. 193–202, 2004.

[35] R. Davis and J. E. M. Johnston, “The Surge Characteristics of Tower and Tower-Footing,” *Journal of the Institution of Electrical Engineers-Part II: Power Engineering*, vol. 88, no. 5, 1941.

[36] S. Visacro, “A comprehensive approach to the grounding response to lightning

currents," *IEEE Transactions on Power Delivery*, vol. 22, no. 1, pp. 381–386, 2007.

[37] K. J. Nixon, "The Lightning Transient Behaviour of a Driven Rod Earth Electrode in Multi-Layer Soil - PhD Thesis," University of the Witwatersrand, Johannesburg, 2006.

[38] S. Sekioka, "Discussion of Current Dependent Grounding Resistance using an Equivalent Circuit Considering Frequency-dependent Soil Parameters," in *International Conference on Lightning Protection*, 2016.

[39] S. Sekioka, M. I. Lorentzou, and N. D. Hatziargyriou, "Approximate formulas for terminal voltages on the grounding conductor," *IEEE Transactions on Electromagnetic Compatibility*, vol. 56, no. 2, pp. 444–453, 2014.

[40] IEEE Standards Assocation, "IEEE Guide for Improving the Lightning Performance of Electric Power Overhead Distribution Lines," 2010.

[41] R. Alipio and S. Visacro, "Frequency dependence of soil parameters: Effect on the lightning response of grounding electrodes," *IEEE Transactions on Electromagnetic Compatibility*, vol. 55, no. 1, pp. 132–139, 2013.

[42] W. A. Chisholm, "Evaluation of Simple Models for the Resistance of Solid and Wire-Frame Electrodes," *IEEE Transactions on Industry Applications*, vol. 51, no. 6, pp. 5123–5129, 2015.

[43] V. P. Androvitsaneas, I. F. Gonos, and I. A. Stathopulos, "Experimental study on transient impedance of grounding rods encased in ground enhancing compounds," *Electric Power Systems Research*, vol. 139, pp. 109–115, 2016.

[44] CIGRE Working Group C4.407, "Lightning Parameters for Engineering Applications," 2013.

[45] S.Sekioka, T. Hara, and A. Ametani, "Development of a nonlinear model of a concrete pole grounding resistance," in *International Conference on Power*

Systems Transients (IPST'05), 1995.

[46] W. Gamerota, J. Elism, M. Uman, and V. Rakov, "Current Waveforms for Lightning Simulation," *IEEE Transactions on Electromagnetic Compatibility*, vol. 54, no. 4, pp. 880–888, 2012.

[47] M. A. O. Schroeder, M. T. C. De Barros, A. C. S. Lima, M. M. Afonso, and R. A. R. Moura, "Evaluation of the impact of different frequency dependent soil models on lightning overvoltages," *Electric Power Systems Research*, 2017.